

## Single-particle study of protein assembly

Ching-Hwa Kiang

*Physics Department, University of California, Los Angeles, California 90095*

(Received 14 December 2000; revised manuscript received 15 June 2001; published 24 September 2001)

A study of protein assembly in solution with single-particle imaging and reconstruction techniques using cryoelectron microscopy is reported. The human glutamine synthetase enzyme, important in brain metabolism, and previously assumed to be assembled into a homogeneous quaternary structure, is found to be heterogeneous, with three oligomeric states that co-exist at room temperature. This result corrects an old structural and kinetic model determined by ensemble averaging techniques that assumed a homogeneous system. Unexpectedly fast protein dissociation kinetics results from a stabilized transition state.

DOI: 10.1103/PhysRevE.64.041911

PACS number(s): 87.15.-v, 03.65.Ta, 89.70.+c

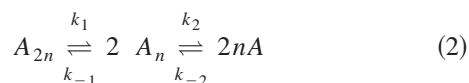
Protein folding and assembly is of general interest in biophysics. Equilibrium and transient protein structures provide valuable information about the folding processes. Multiple transition states resulting from a complex free energy landscape for protein folding and assembly have been investigated theoretically [1,2]. The complexity of biological macromolecules makes single-particle experiments particularly useful in obtaining dynamic [3] and kinetic [4] information. Single-particle cryoelectron microscopy has been used in solving biological macromolecule structures [5], and the technique is suitable for investigating multiple-phase systems [6]. Structural information, when combined with kinetic data on conformational changes [7], yields much information on the dynamics of biological molecules in solution. To explore the enzyme assembly process *in vitro*, we study the glutamine synthetase (GS) dissociation-association pathway using single-particle cryoelectron microscopy.

GS is an enzyme ubiquitous in human cells, and malfunction of GS has been found to play an important role in disease, neuronal degeneration after injury, and the aging processes. There are two forms of GS, GSI and GSII. GSI is a stable 12-subunit assembly found only in prokaryotes (e.g., bacteria and blue-green algae), with a monomer molecular weight of 52 kDa [8,9]. GSII is also a large assembly found in eukaryotes (e.g. plants and mammals), with a monomer molecular weight in the range of 39–47 kDa [10,11]. Human GS (GSII) and bacterial GS (GSI) differ in the amino acid sequences, the number of subunits, and the regulation mechanisms [9,12–14]. Understanding the difference between GSI and GSII is of great medical importance and may shed light on enzyme evolution.

Subunit assembly of GS is used to regulate enzymatic activities. The equilibrium of GSI involves only two states



whereas the reaction pathway of GSII involves a metastable state in the transition state



(see Fig. 1). The rate constant  $k$  is described with Arrhenius

equation

$$k = k_0 e^{-E_a/RT} \quad (3)$$

where  $k_0$  is the preexponential factor and  $E_a$  is the free energy of activation. The activation energy of GSII,  $E_a$ , is smaller than that of GSI,  $E'_a$ , and a decrease of 2.73 kcal/mol in  $E_a$  results in a 100 fold greater  $k$  at room temperature. The equilibrium constant  $K_{eq}$  of  $A_{2n} \overset{k_1}{\rightleftharpoons} 2 A_n \overset{k_{-1}}{\rightleftharpoons} A_{2n}$  was measured to be  $2.5 \times 10^{-6}$  M [14] at 37 °C, and therefore, at an initial 1 mg/ml concentration of  $A_{2n}$ , the equilibrium composition of  $A_n/A_{2n}$  is 2/3. Using

$$\Delta G^\circ = -RT \ln K_{eq},$$

the free energy difference between  $A_{2n}$  and  $A_n$  is estimated to be 8 kcal/mol at 37 °C.

Human GS was prepared with recombinant DNA technology and expressed in *E. Coli*. We imaged human GS with a JEOL1210 transmission electron microscope equipped with a Gatan cold stage. The microscope was operated at 120 kV acceleration voltage. Frozen hydrated specimens were prepared in a humidity controlled freezing apparatus. A drop of

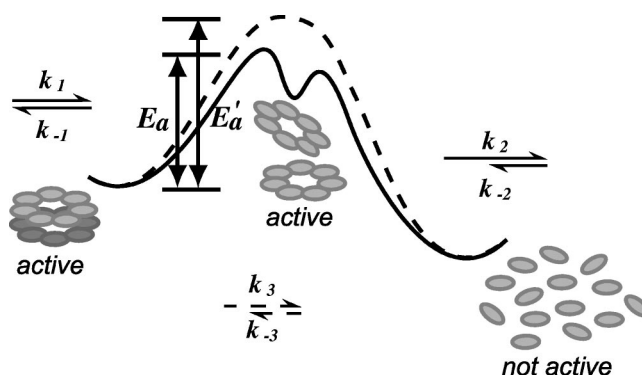


FIG. 1. Dissociation pathways of GS. Solid line: mammalian GS (GSII), dashed line: bacterial GS (GSI). The activation energy  $E'_a$  of GSI is high, which results in a smaller  $k_3$ , whereas the  $E_a$  of GSII is lowered owing to a metastable species that is not observed for GSI. The rate constant of the rate-limiting step  $k_1$  is significant at room temperature. Note that GSII is a tetradecamer, as shown, whereas GSI is a dodecamer.

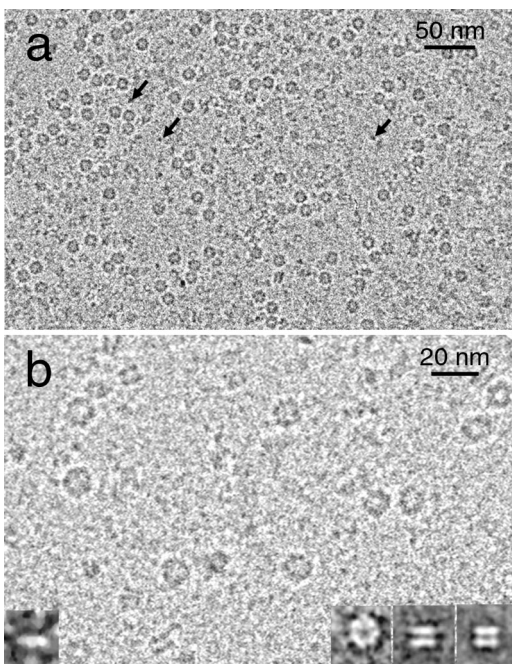


FIG. 2. (a) Unprocessed cryoelectron microscopy images of human GS. Solution containing 1 mg/ml human GS in 5 mM MgOAc, 1 mM TIOAc, and 25 mM Hepes buffer pH=6.8 was put on a lacey carbon grid. Images were taken at a magnification of 30000 with a defocus between 0.5 and 0.9  $\mu\text{m}$  and captured with a charge-coupled device (CCD) camera at a resolution of 5.3  $\text{\AA}$  per pixel. The exposure times were kept between 1 and 2 seconds to ensure the electron dose was less than 10 electrons per  $\text{\AA}^2$ . The arrows point to some of the monomers embedded in the ice film, indicating the heterogeneity in the system. (b) Two orientations dominate in the micrograph. The top views indicate a seven fold symmetry, and the side views display a double-layered structure. Inset: noise-filtered views of single particles from different Euler angles showing the typical one-layer (left) or two-layer (right) structure and seven subunits. The gray scale level has been reversed for reconstruction and display purposes.

2  $\mu\text{l}$  solution was blotted from the back of the film for 3–5 s and plunged into liquid ethane (cooled in liquid nitrogen bath) to ensure formation of a thin layer of vitreous ice. The cooling rate was  $\sim 100\,000$   $^{\circ}\text{C}/\text{s}$ . The sample was then transferred to a Gatan cryotransfer stage and inserted into a cryospecimen holder maintaining the sample at  $-180$   $^{\circ}\text{C}$ .

Figure 2(a,b) is an unstained cryoelectron microscopy image of human GS embedded in vitreous ice. GSII particles were manually picked and boxed in 272  $\text{\AA}$  by 272  $\text{\AA}$  windows (51 by 51 pixels), as shown in inset of Fig. 2(b). The side projections were rotated and shifted within the window prior to correlation averaging [Fig. 3(a)]. The top projections were also averaged according to the cross-correlation function with no imposed symmetry, and the result shows a seven-fold symmetry [Fig. 3(b)]. A three-dimensional structure, reconstructed using weighted-back-projection [5,15,16], is shown in Figs. 3(c). The model demonstrates that human GS is composed of a pair of heptamer rings of diameter 140  $\text{\AA}$  and an overall height of 100  $\text{\AA}$ , with a central channel of 40  $\text{\AA}$  diameter. The neighboring active sites within

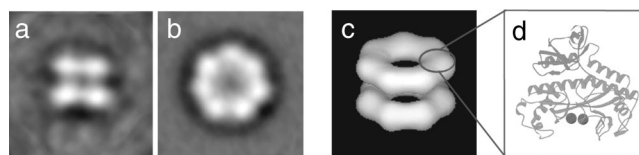


FIG. 3. Correlation averaged side view (a) and top view (b) show the typical two-layered density and sevenfold symmetry, respectively. Particle alignment and averaging were done by reference-free, interactive cross correlation, using the algorithms written for the SPIDER [17] and EMAN [18] softwares. The information is significant to  $\sim 25$   $\text{\AA}$ , which was assessed by splitting the data set in half and computing the Fourier shell correlation coefficient. (c) Surface rendered representation of the three-dimensional structure of human GS reconstructed with an imposed sevenfold symmetry as determined by the two-dimensional electron microscopy image (b). (d) Monomer structure of human GS obtained from homology modeling, using the crystal structure of monomer GSI [9] as template. The GS monomer has no enzymatic activity because the active sites are between subunits.

the same ring of seven subunits are separated by 45  $\text{\AA}$ . The overall dimension of human GS (GSII) is similar to that of GSI, which is a dodecamer with two hexamer rings arranged into an oligomer 140  $\text{\AA}$  wide and 100  $\text{\AA}$  high [9].

To verify the accuracy of the reconstruction, we used the same technique to collect cryoelectron microscopy images and determine the structure of *Salmonella* GS (GSI). Pure *Salmonella* GS exists in a single oligomeric form, as shown in Fig. 4. A reconstructed three-dimensional model shows GSI is composed of 12 subunits with a sixfold symmetry, in agreement with x-ray crystal structure results [9] and confirming the validity of our approach.

GSII was estimated to be an octamer for over 40 years. This confusion arose from ensemble measurements of mo-

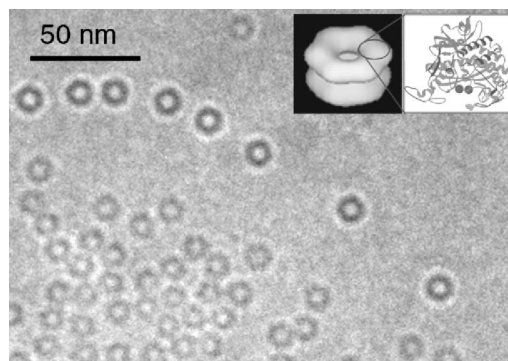


FIG. 4. Cryoelectron microscopy image of frozen hydrated *Salmonella* GS. The sample is homogeneous, as the enzyme exists in a single, stable oligomeric state. The electron beam focus was adjusted to be far underfocused to enhance image contrast [19], which minimizes the number of particles required for reconstruction at this resolution. Inset is the reconstructed three-dimensional model of GSI and the x-ray structure of the GSI monomer [9]. The structure is reconstructed from two distinct angles, where top view was averaged over ten particles, and the side view was from a single image. The small amount of image data necessary for reconstruction by cryoelectron microscopy is advantageous for studying heterogeneous systems.

lecular weight and the often confusing negative staining electron microscopy images [20,21]. Indeed, interpretations of analytical ultracentrifugation, gel filtration, and negative staining electron microscopy studies of oligomeric proteins are often ambiguous [22]. Molecular weight measurements for GSII range from 384 kDa to 525 kDa [20,21,23], and the oligomeric state was incorrectly chosen to be 8 subunits. As shown in Fig. 1, lowering free energy barrier increases reaction rates, which results in reaching the equilibrium state at a faster rate. In the case of GSII, ensemble measurement cannot be completed before significant dissociation occurs, and significant amounts of monomer  $A$  and heptmer  $A_7$  are responsible for the variety and reduced values of the GSII molecular weight. This suggestion is supported by comparing the cryoelectron micrographs of GSI and GSII, which show that the solution of GSI contains almost no monomer, in contrast to the large amount of monomer present in GSII solution. Taking 14 to be the fully assembled oligomeric state, the averaged molecular weight measured by ensemble techniques, 400 kDa, corresponds to a composition of 50%  $A_{14}$ , 30%  $A_7$ , and 20%  $A$ .

Homology modeling of GSII indicates that a tetramer would have an open structure, which is less favorable than a closed form [24]. Because GSI and GSII have 30% sequence identity, it is nearly impossible to construct a heterologous tetramer of GSII without significantly altering the tertiary structure of the subunits, which is disfavored since it would very likely result in a higher energy structure. Moreover, Monod *et al.* has pointed out that one major reason for an oligomeric enzyme to be large compared to the stereospecific active site is that this allows residues to be fixed in a precise

orientation that altogether composes a stereospecific site [24]. Through molecular evolution, the number of residues required to fix a specific active sites configuration should be minimized, which may be achieved by increasing the number of subunits in an oligomer while decreasing the monomer molecular weight. This is consistent with the finding that the GSI is composed of 12 subunits (molecular weight=52 × 12=624 kDa) while GSII has 14 subunits (molecular weight=42 × 14=588 kDa).

Using single-particle imaging and reconstruction, we have observed heterogeneity of protein assembly, GSII, and conclude that the fast dissociation kinetics of GSII is responsible for the reduced apparent molecular weights previously observed. We have also identified a seven fold symmetry in the electron density map, and reconstructed a three-dimensional model of GSII that shows a 14-subunit arrangement. It has been suggested that GroE chaperonins facilitate GS folding and assembly by eliminating misfolded intermediate states and by controlling the off-pathway kinetics [25], which explains the unexpectedly fast GSII enzyme dissociation kinetics *in vitro*. Our results suggest that the data deduced for GSII based on the assumption of an octameric structure must be reanalyzed and reinterpreted. Further investigation of protein folding and assembly dynamics and kinetics is necessary to understand the complex enzymatic activities of heterogeneous systems such as the one studied here.

We thank David Eisenberg, Gaston Pfluegl, and Tieu Phung for helpful discussions and for providing GS samples. This research was supported by NIH Grant No. 1R03AG15626-01.

- 
- [1] S. Takada and P.G. Wolynes, Phys. Rev. E **55**, 4562 (1997).  
 [2] J.J. Portman, S. Takada, and P.G. Wolynes, Phys. Rev. Lett. **81**, 5237 (1998).  
 [3] J. Nardi, R. Bruinsma, and E. Sackmann, Phys. Rev. Lett. **82**, 5168 (1999).  
 [4] X. Zhuang *et al.* Science **288**, 2048 (2000).  
 [5] B. Böttcher, S.A. Wynne, and R.A. Crowther, Nature (London) **386**, 88 (1997).  
 [6] S. Chiruvolu *et al.*, Science **266**, 1222 (1994).  
 [7] N.L. Goddard, G. Bonnet, O. Krichevsky, and A. Libchaber, Phys. Rev. Lett. **85**, 2400 (2000).  
 [8] A. Ginsburg and E. R. Stadtman, in *The Enzymes of Glutamine Metabolism*, edited by S. Prusiner and E. R. Stadtman (Academic Press, New York, 1973), pp. 9–43.  
 [9] R.J. Almassy *et al.*, Nature (London) **323**, 304 (1986).  
 [10] A. Meister, Methods Enzymol. **113**, 185 (1985).  
 [11] A.V. Pushkin *et al.*, Biochim. Biophys. Acta **828**, 336 (1985).  
 [12] L. Stryer, *Biochemistry* (Freeman, New York, 1995).  
 [13] *The Enzymes of Glutamine Metabolism*, edited by S. Prusiner and E. R. Stadtman (Academic Press, New York, 1973).  
 [14] F.C. Wedler, R.B. Denman, and W.G. Roby, Biochemistry **21**, 6389 (1982).  
 [15] J. Frank *et al.*, Nature (London) **376**, 441 (1995).  
 [16] S. Chen *et al.*, Nature (London) **371**, 261 (1994).  
 [17] *Three-Dimensional Electron Microscopy of Macromolecular Assemblies*, edited by J. Frank (Academic Press, New York, 1996).  
 [18] S.J. Ludtke, P.R. Baldwin, and W. Chiu, J. Struct. Biol. **128**, 82 (1999).  
 [19] *High-Resolution Transmission Electron Microscopy and Associated Techniques*, edited by P. R. Buseck, J. M. Cowley, and L. Eyring (Oxford University Press, New York, 1988).  
 [20] R.H. Haschemeyer, Trans. N. Y. Acad. Sci. **30**, 875 (1968).  
 [21] J. Stahl and L. Jaenicke, J. Biochem. **29**, 401 (1972).  
 [22] J.E. Gouaux *et al.*, Proc. Natl. Acad. Sci. U.S.A. **91**, 12828 (1994).  
 [23] V. Pamiljans, P.R. Krishnaswamy, G. Dumville, and A. Meister, Biochemistry **1**, 153 (1962).  
 [24] J. Monod, J. Wyman, and J.-P. Changeux, J. Mol. Biol. **12**, 88 (1965).  
 [25] M.T. Fisher, Biochemistry (Mosc) **63**, 382 (1998).